Loss Consideration of Magnetic Fault Current Limiter

Loss Consideration of Magnetic Fault Current Limiter

K. Yotsutsuji[1], M. Kitazawa[1], S. Yamada[2] and M. Iwahara[1]
[1] Graduate School of Natural Science and Technology, Kanazawa University
[2] Division of Biological Measurement and Applications, Institute of Nature and Environmental Technology, Kanazawa University

Current suppression devices such as fault current limiter (FCL), which have high impedance under fault conditions and low impedance under normal conditions, are required to reduce excessive current in power distribution lines, when fault such as short circuits occurs in large scale electric power systems. In this paper, to establish practical design method of magnetic FCL, the design and the characteristics of a prototype magnetic FCL of 2 kVA order are investigated. And the loss mechanism of magnetic FCL is discussed for getting better the line current suppression characteristics.

Key Words: magnetic fault current limiter, three leg core, permanent magnet, loss analysis

1. Introduction

Power distribution system has been expanded continuously into a wide and a large scale due to its easy energy conversion abilities, and its power consumption is also growing up rapidly. In addition, many of the information equipment are used at any time and all days recently. In these situations, the power distribution system is demanded to supply the power with no interrupt and a high stability at any of time. One of methods to answer to these demands, Fault Current Limiter (FCL) is employing [1 and 2] for the purpose of preventing fault current and conserving the system facilities in any case of accidents happened. Supposing the FCL for low-voltage distribution systems, we have had developed a magnetic FCL, which is a full passive and is made of coils and a compound core only with a permanent magnet [3]. For confirming the practical design of it, we need to analyse the loss of this device. In this paper, we report the consequence of characteristic evaluation, B-H loop which is obtained by the voltage waveforms in this device and characteristics of loss in the magnetic FCL of 2 kVA order for distribution systems.

2. Principles and Operating Point of Magnetic Fault Current Limiter

2.1 Principles and operating point

The FCL is inserted in series to the distribution systems as shown in Fig.1. The required characteristics of current limiter is shown in Fig.2. Under the normal condition, it has low impedance, and allows a current without any of voltage drop, but it has high impedance and limits to a small current instantly when a large value of fault current flows in the circuit. As shown in Fig.3, the magnetic FCL includes a permanent magnet in the central leg of the core and is wounded with two conductive wires in each of side legs. The operating point P of this magnetic FCL is determined by the intersected point of the magnetic characteristic of permanent magnet (solid line: linear approximation) and of the whole core (broken line: bi-sectional lines approximation) shown in Fig.4. As this device operates at the point P, this point strongly affects to the design of magnetic FCL. For this reason, the performance of this device should be treated by the nonlinear analysis. In Fig. 4, $\Delta\phi$ shows the shaped width of flux which can be used in magnetic FCL.

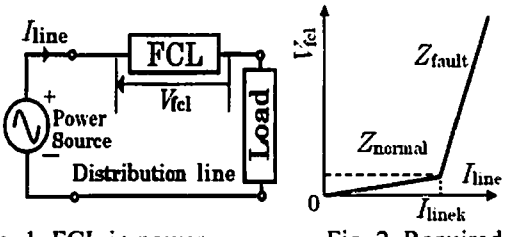

Fig. 1 FCL in power distribution line.

Fig. 2 Required characteristics of FCL.

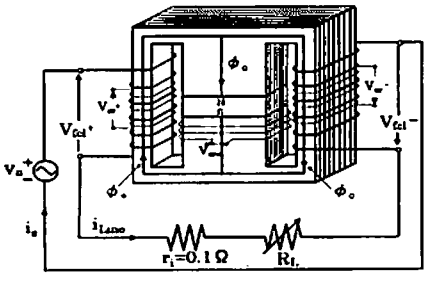

Fig. 3 Configuration of FCL.

Correspondence: M. Iwahara, Graduate School of Natural Science and Technology, Kanazawa Univ., Kakuma-machi, Kanazawa, Ishikawa 920-1192, Japan
email: iwahara@magstar.ec.t.kanazawa-u.ac.jp

And then the maximum voltage V_{fclm} [V] in magnetic FCL is expressed as follows,

$$V_{fclm} = N\omega\Delta\phi \quad (1)$$

N: Number of turns, ω: Angular frequency [rad.].

If $\Delta\phi$ can be a larger, the terminal voltage of magnetic FCL is a larger, and then the rate of current limiting is increasing. ΔU is the shaped width of magneto-motive force at the starting point of current limit in the magnetic FCL, and its relational expression as follows,

$$NI_{Line} = \Delta U \quad (2)$$

Magnetic FCL is operated alternatively at the point P. Waveforms of V_{fcl} and I_{Line} are able to estimate by using the biased bi-sectional line. That is, the line current i_{Line} is not reduced by the FCl at below the I_{Linek} (broken line) as shown in Fig.5. When the FCL operates at over i_{LineK}, i_{Line} is reduced by the FCL (solid line). In these waves shown in Fig.6, the terminal voltage V_{fcl} is greatly increasing as it has high impedance in the region of limiting the current ($\theta_k < \theta < \pi - \theta_k$). On the other hand, it has low impedance in the region where the current is not limited ($\theta < \theta_k$, or $\pi - \theta_k < \theta$), and then it is negligible small of line drop.

3. Prototype and the Method of Experiment

3.1 Prototype of the Magnetic FCL

The prototype FCL has been designed for the distribution system of the line voltage 100V, and line current 10A. The number of coil turns and the geometry of the magnetic core are decided by calculating the operating point P to realize the desirable characteristics. The model is shown in Fig.7 for the FEM analysis using the Maxwell SV (by Ansoft) and the calculation of operating point P. Fig.8 shows the FCL device setup. The magnetic characteristic of core material is shown in Fig.9, and the material parameters, H_c: Coercive force of magnet, B_r: Residual flux density of magnet, B_k: Knee point flux density of core, μ_{ru}, μ_{rs}: Relative permeability of unsaturated and saturated regions of core respectively are shown in Table I. The result of FEM analysis with the auto-mesh and without the line current is shown in Fig.10. It is shown that both legs are sufficiently biased to the saturated region of core. As the result, the operating point P is calculated as shown in Fig.11. From Fig.11, ΔU=4000AT, and we can predict that the current I_{Linek} is 13.3A if the number of coil turns is assumed to N_{fcl+}=N_{fcl-}=150 turns. The turns N_{sr+} , N_{sr-} of search-coils are 10 turns each.

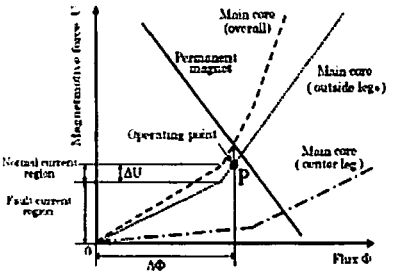

Fig. 4 Biased operating point.

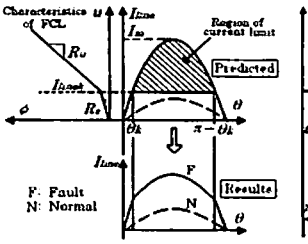

Fig. 5 Waveforms of line current.

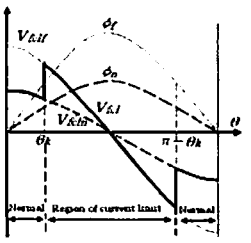

Fig. 6 Waveforms of the V_{fcl}.

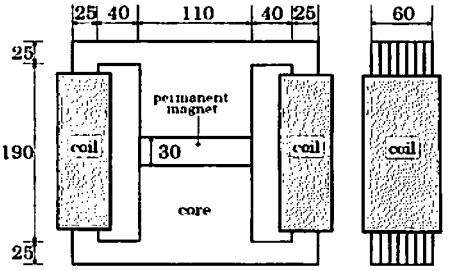

Fig. 7 Dimensions of FCL core.

Table I: Material parameters.
(a) Permanent magnet. (b) Core (with lines).

H_c [kA/m]	855
B_r [T]	1.29

B_k [T]	1.5
μ_{ru}	4800
μ_{rs}	100

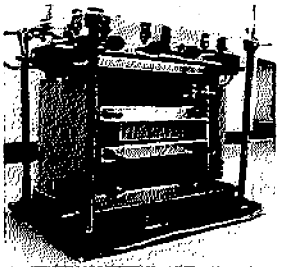

Fig. 8 Photograph of FCL.

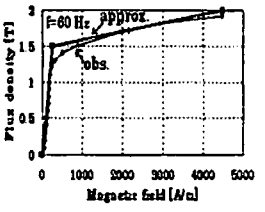

Fig. 9 Magnetic characteristics of core.

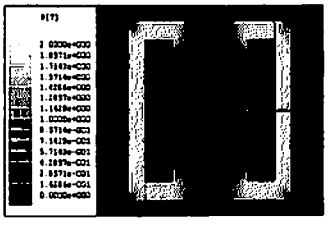

Fig. 10 Magnetic flux density of the FCL core.

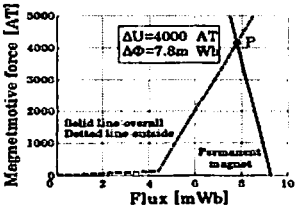

Fig.11 Operating point biased by the magnet.

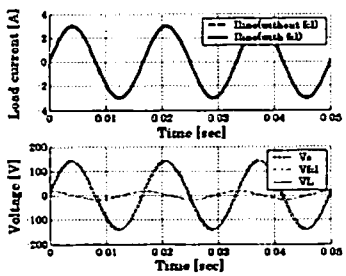

Fig. 12 Waveforms of FCL under normal condition.

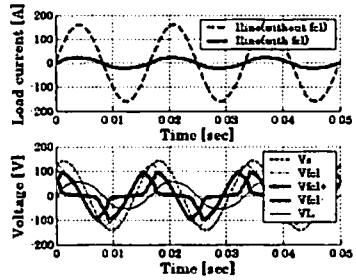

Fig. 13 Waveforms of FCL under fault condition.

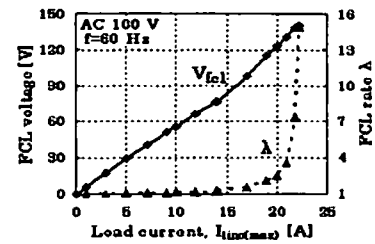

Fig. 14 Characteristic of FCL and FCL limiting rate.

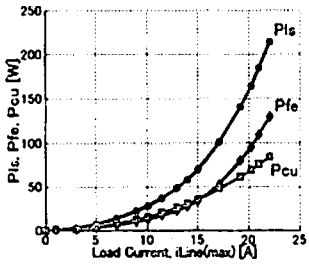

Fig. 15 Characteristics of the loss versus the line current.

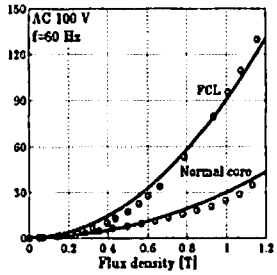

Fig. 16 Characteristic of Iron loss versus B_{rms}.

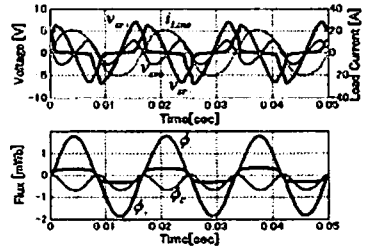

Fig. 17 Search coil voltage, current and flux waveforms of FCL under fault condition.

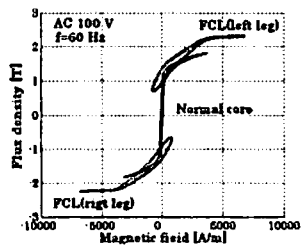

Fig. 18 B-H loop of FCL superposed on normal core's B-H loop.

3.2 Waveforms and the Characteristics of the FCL

In order to inspect the result of numerical analysis, the experiments was done by the circuit in Fig.3 with frequency f =60Hz, and supply voltage V_s=100V, varying the load R_L. The waveforms of the V_{fcl} and I_{Line} are shown in Fig.12 and Fig.13. The terminal voltage of FCL is not large and the current is normal under the normal condition. On the other hand, under the fault current condition, the FCL absorbs most of the power supply voltage, and the current is kept in low. And terminal voltages V_{fcl+}, V_{fcl-} at both legs of FCL are similar with the estimated waveforms shown in Fig.6.

The performance of FCL has been evaluated with the limiting rate λ defined by Eq. (3).

$$\lambda = I_{withoutFCL} / I_{withFCL} \tag{3}$$

$I_{withoutFCL}$: the current without FCL [A]
$I_{withFCL}$: the current with FCL [A]

The characteristics of FCL and the limiting rate are shown in Fig.14. Although the performance of FCL in Fig.14 is insufficiency rather than that of Fig.2, but it shows that the FCL impedance shifts from low impedance to high impedance at around 14 A. This break point nearly equals the design value 13.3 A. And the FCL limiting rate λ increased from the break point and it becames as high as 15 at the I_{Line}=22 A.

3.3 The Characteristics of FCL Loss

The iron loss behaviour and its characteristics have been discussed by the operating mechanism. As the core is magnetized by a permanent magnet, and the operating waveforms are complicated, it is not easy to measure the loss by the usual method. The terminal voltage of FCL: V_{fcl}, the induced voltage at the side legs with search-coils: V_{sr+}, V_{sr-}, and the line current I_{Line} was measured. These measurements had been done by using of digital waveform memory with 12 bits resolution. And then the loss is calculated with the digital data based on Eq. (4) as below,

$$\left.\begin{aligned} P_{ls} &= \frac{1}{T}\int_0^T V_{fcl}\cdot i_{line}\,dt \\ P_{fe} &= \frac{1}{T}\int_0^T \frac{N_{fcl}}{N_{sr}}(v_{sr+}+v_{sr-})\cdot i_{line}\,dt \\ P_{cu} &= P_{ls} - P_{fe} \end{aligned}\right\} \tag{4}$$

P_{ls}: Total loss [W], P_{fe}: Iron loss [W], P_{cu}: Copper loss [W], T: period of the voltage and current [Sec]

The iron loss is a bigger than the copper loss at that the FCL governs the fault current. Fig.16 shows a comparison between the FCL's and the normal core's iron losses. Here, it is called a normal core, when the magnetic core of FCL is used as a reactor. Comparing both characteristics of iron loss, the iron loss of the FCL is 3.3 times lager than that of the normal core. This result shows there is a different loss mechanism in the FCL 's operation.

4. Dependence of the Loss in the Characteristics of the FCL

4. Dependence of the Loss in the Characteristics of the FCL

4.1 The B-H loop of FCL

Figure 17 shows the waveforms of the induced voltage in a search-coil, the line current, and the flux which is numerically integrated from the induced voltage. The B-H loop of FCL is obtained from the flux and the line current waveforms. Using the FEM analysis, the B-H loop of FCL is superimposed on the B-H loop of the normal core as shown in Fig.18. The B-H loop in Fig.18 is different from the generally known B-H loop. The differences are; (i) B-H loop width is increasing rather than that of normal core B-H loop, (ii) B-H loop gradient is gradual rather than that of normal core B-H loop. (iii) B-H loop shifts the B-H loop of the normal core. Based on these results, we can discuss the reason why the performance of FCL is insufficient. That is, the insufficient performance is caused by (i), and by iron loss being larger which is caused by (ii), (iii). And as this FCL is magnetized sufficiently to the saturated region, the differences (ii), (iii) are caused by the flux flowing in the central leg from the side leg, and the leakage flux being larger. And moreover as the flux flows in the magnet, eddy current occurs in the magnet. This is affecting to the large width of FCL B-H loop.

4.2 The Effect of Eddy Current

Although the iron loss of core is affected by the eddy current in the permanent magnet of the central leg, it is difficult to measure directly the eddy current in the magnet. Then it is assumed that the eddy current in the magnet flows intensively in the short-circuit coil n_c (5 turns) which is fixed at the central leg, and the effect of the eddy current on the FCL B-H loop is estimated in Fig.19. The line current i_{Line} includes the component of eddy current i_{dc} which flows at the short-circuit coil times n_c / N_{fcl}. As the eddy current i_{dc} is included in the FCL's B-H loop, the effect of the eddy current should be eliminated from the line current as below

$$I_{Line} = i_{Line} - i_{dc} n_c / N_{fcl} \quad (5)$$

At the i_{line}(max) =20A, the waveforms of the voltage, the load current and the eddy current in the short-current coil, which has been measured by CT probe (HIOKI 3274), is shown in Fig.20. The waveforms of the eddy current i_{dc} in the short-current coil are similar to the 2nd harmonics of V_{src}, and the amplitude of the eddy current is 50 A. The B-H loop of FCL without the effect of eddy current is shown Fig.21.And it is shown that the B-H loop

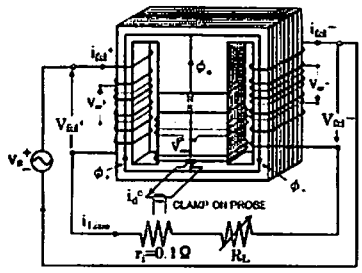

Fig. 19 Experimental circuit.

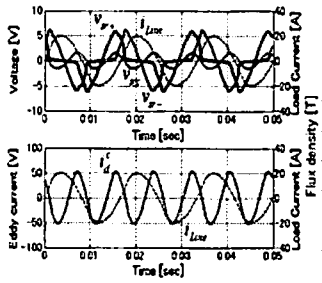

Fig. 20 Waveforms of eddy current.

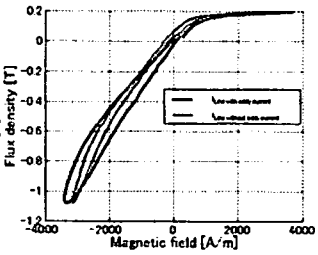

Fig. 21 FCL B-H loop eliminated eddy current.

width of FCL becomes narrow. Hence, it is said that the wide width of B-H loop is caused the eddy current, and the iron loss of the FCL is larger than that of the normal core due to eddy current.

5. Conclusion

The prototype magnetic FCL of 2kVA order has been investigated on that current limit performance and loss mechanism. The iron loss of FCL is increasing with the square of the flux density as well known, but the iron loss is 3.3 times larger than that of the normal core. From the obtained B-H loop, it is clear that the flux which flows in the center leg and the leakage flux is a larger. In addition, it is considered that the iron loss is increasing by eddy current which occurs as a result of flux flowing in the center leg. And then the performance of FCL depends on the flux distribution and the loss.

References

[1] Standstill device technology committee of IEEJ Trans. Power and Energy: Present Conditions and Prospects of Fault Current Limiting Technology, *Technology report of IEEJ*, No.850, 2001.

[2] H. Shimizu, "Current State and Trends of Fault Current Limiting Technology," *IEEJ Trans. Power and Energy*, No.125, 2005.

[3] H. Nakamichi, K. Yotsutsuji, S. Yamada and M. Iwahara, "Numerical Analysis of the Core Dimensions of a Magnetic FCL Assuming a Practical Design and Trial Production," *Journal of MSJ*, Vol.30, No.2, pp. 282-285, 2006.